Supplemental Material for

"Edge currents as a signature of flat bands in topological superconductors"

Authors: Andreas P. Schnyder, Carsten Timm, and P. M. R. Brydon

For completeness, we present in this Supplement Material the z component of the spin-LDOS at the edge of an NCS. We also study the changes in the edge band structure induced by a z-polarized exchange field in the leading edge of the NCS and determine the resulting edge currents. The results are qualitatively similar to the ones for an x-polarized exchange field, which we have discussed in the main text.

I. EDGE BAND STRUCTURE

Fig. S1 displays the z component of the energy- and momentum-resolved spin-LDOS for the outermost layer at the (10) edge of the $(d_{xy}+p)$-wave and $(s+p)$-wave NCS. This figure should be compared to the x component of the momentum-resolved spin-LDOS, which is depicted in Figs. 1(b), (d), (f), and (h) of the main text. As stated in the main text, both the continuum and subgap states have a strong total spin polarization in the xz spin-plane. As required by time-reversal symmetry, the total spin polarization is an odd function of edge momentum k_y. The nondegenerate zero-energy flat bands of the $(d_{xy}+p)$-wave NCS show a particularly strong and robust x-spin polarization [Figs. 1(b) and (d)], with a weaker z-spin polarization that changes sign near $\pm(k_{F,-}-k_{F,+})/2$ [Figs. S1(a) and (b)]. The doubly degenerate states of the $(d_{xy}+p)$-wave NCS, which appear in the region $|k_y| \in [k_{F,+}, k_{F,-}]$, give opposite contributions to the spin-LDOS of unequal magnitude. They therefore exhibit a weaker overall spin polarization than the nondegenerate states [Figs. 1(d) and S1(b)].

An exchange field applied to the leading edge of a $(d_{xy}+p)$-wave NCS turns the nondegenerate flat bands into dispersing chiral modes. We have demonstrated this for an x-polarized exchange field in Figs. 2(a) and (b) of the main text. Figs. S2(a) and (b) show the corresponding results for an exchange field polarized along the z axis. As before, we find that the exchange field $\mathbf{H}_{\rm ex} = 0.4\,\mathbf{e}_z$ leads to an energy shift of the edge states which is proportional to $H^z_{\rm ex}\,\rho^z_1(E,k_y)$. Finally, also the left- and right-moving edge states of the $(s+p)$-wave NCS are shifted in energy due to the proximity-induced exchange field, see Fig. S2(c) and compare with Fig. 2(c) in the main text.

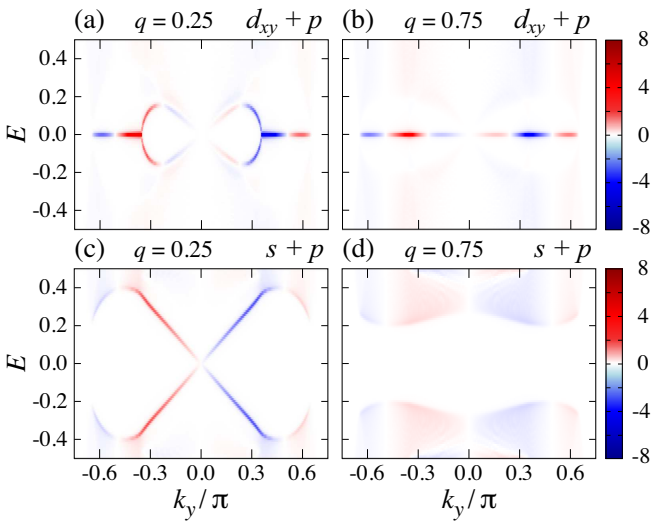

FIG. S1. z component of the energy- and momentum-resolved spin-LDOS for the outermost layer of the $(d_{xy}+p)$-wave NCS with (a) $q = 0.25$ and (b) $q = 0.75$, and for the $(s+p)$-wave NCS with (c) $q = 0.25$ and (d) $q = 0.75$. As in Fig. 1 of the main text the spin-LDOS is plotted in units of $\hbar/20$ on a linear scale.

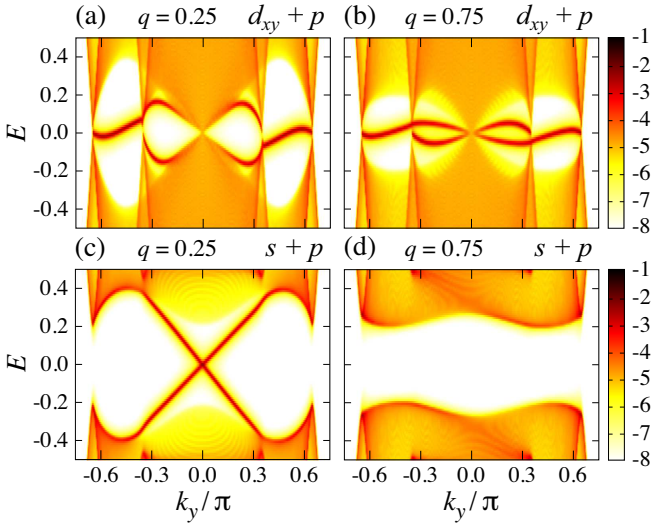

FIG. S2. Energy- and momentum-resolved LDOS on a log scale for the ten outermost layers at the (10) edge of (a), (b) the $(d_{xy}+p)$-wave and (c), (d) the $(s+p)$-wave NCS in the presence of a z-polarized exchange field in the leading edge with $\mathbf{H}_{\rm ex} = 0.4\,\mathbf{e}_z$. In the left column we plot the results for $q = 0.25$ (majority singlet), whereas in the right column we have $q = 0.75$ (majority triplet).

II. EDGE CURRENTS

As explained in the main text, the energy shifts of the edge states induced by the exchange field lead to a spontaneous current at the edge of the NCS. We have exemplified this for an x-polarized exchange field in Fig. 3 of the

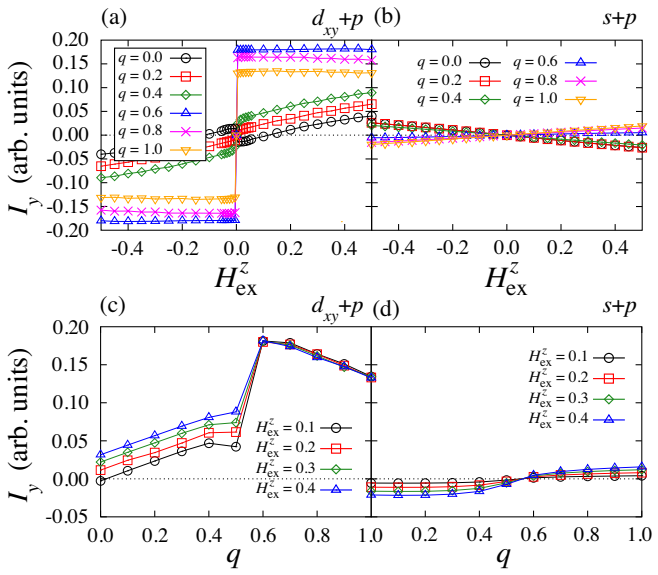

FIG. S3. Top row: Edge current I_y as a function of exchange field $\mathbf{H}_{\rm ex} = H_{\rm ex}^z \mathbf{e}_z$ for various values of the singlet-triplet parameter q for (a) the $(d_{xy}+p)$-wave and (b) the $(s+p)$-wave NCS. Bottom row: Edge current I_y as a function of singlet-triplet parameter q for various values of the exchange field $\mathbf{H}_{\rm ex} = H_{\rm ex}^z \mathbf{e}_z$ applied to the edge layer of (c) the $(d_{xy}+p)$-wave and (d) the $(s+p)$-wave NCS.

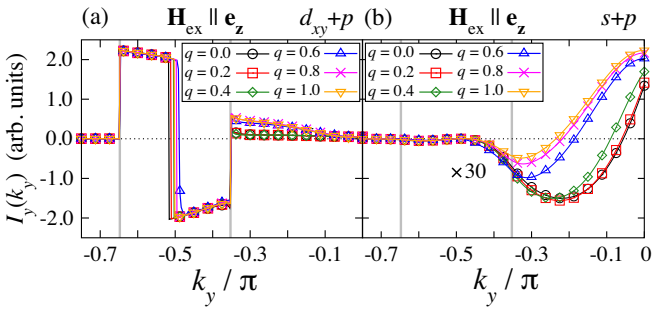

FIG. S4. Momentum-resolved edge current $I_y(k_y)$ for various values of singlet-triplet parameter q in (a) the $(d_{xy}+p)$-wave and (b) the $(s+p)$-wave NCS in the presence of an exchange field $\mathbf{H}_{\rm ex} = 0.2\,\mathbf{e}_z$ applied to the edge layer. The current in the $(s+p)$-wave case has been multiplied by 30 for better visibility.

main text. In Fig. S3 we present the edge current I_y for a z-polarized exchange field, as a function of singlet-triplet parameter q and exchange field $\mathbf{H}_{\rm ex} = H_{\rm ex}^z \mathbf{e}_z$. Similar to Fig. 3, we find that also a z-polarized exchange field indcues a finite current both for the $(d_{xy}+p)$-wave and the $(s+p)$-wave NCS. As in Fig. 3(a), the current at the edge of the $(d_{xy}+p)$-wave NCS exhibits a singular dependence on exchange-field strength [Fig. S3(a)]. The current at the edge of the $(s+p)$-wave NCS, on the other hand, grows linearly with the exchange field, see Fig. S3(b).

Finally, in Fig. S4 we present the momentum-resolved current $I_y(k_y)$ for an exchange field polarized along the z-axis. The corresponding plot for the x-polarized exchange field is given in Fig. 4 in the main text. Interestingly, for an exchange field along the z axis the current shows a jump in $I_y(k_y)$ at the location of the sign change of the z component of the spin polarization of the non-degenerate edge states, cf. Figs. S1(a) and (b).